




Enhanced Torsion Mechanism of Small-Scale Reinforced Concrete Beams with Spiral Transverse Reinforcement

Shereen Mahmoud ¹, Ahmed Youssef ^{2*}, Hamed Salem ²

¹Department of Civil Engineering, Institute of Aviation Engineering and Technology, Giza, Egypt.

²Department of Structural Engineering, Cairo University, Giza, Egypt.

Received 25 July 2022; Revised 04 October 2022; Accepted 16 October 2022; Published 01 November 2022

Abstract

The nonlinear torsional behaviour of small-scale reinforced concrete (RC) beams with continuous staggered spiral as transverse reinforcement stirrups is experimentally investigated. Twelve miniatures RC beams were tested under torsion load considering the closed shape of stirrups and compared with continuous staggered spiral ones. All miniatures beams were scaled down to be one-eighth the prototype beam size. The main parameters considered in this research are stirrup spacing and its configurations. Small scale RC beams were taken into account in the existing study because of their construction simplicity and financial feasibility. Mortar without coarse aggregate was applied instead of concrete to reduce the size effect of applying small scale models. Ongoing research trials have been carried out to obtain an efficacious approach to boost torsion failure mechanisms because brittle torsion failure of RC structural elements should be avoided. This study emphasized boosted torsion capacity, dissipated energy, and helical crack propagation. During testing, the primary cracking torsion moment, ultimate torsion moment, peak twist angle, and failure mechanism of the beams were inspected. The use of spiral stirrups showed great enhancement of the torsional behaviour of samples. It was observed that using spiral stirrups rather than closed stirrups could result in a substantial increase in torsion capacity and dissipated energy of 87.7% and 89.8%, respectively. As a result, the predicted capacities of the RC beams prototype were estimated in detail, taking account the scale down factor implemented by the authors. Values obtained based on international specifications and guidelines were used to compare the experimental results.

Keywords: Reinforcement (RFT); Reinforced Concrete (RC); Small Scale Modelling (SSM); Torsion Mechanism.

1. Introduction

Torsion failure in RC beams is a brittle failure that should be prevented to enhance structural ductility. Torsion failure creates disastrous failures, requiring the more efficacious investigation methods of designing such beams for torsion. Experimental small - scale models are important in structural engineering. Prototype research is recurrently wasteful or impracticable. SSM are beneficial when studying structure behaviour. The most significant advantages of SSM are the simplicity of cost, the ease with which the sample can be controlled, the time saved when preparing the steel cage, and the cost, which causes a greater demand for scale down modelling. Realizing this problem, a lot of studies were performed on the torsional strength of prototype RC beams using diverse strengthening techniques. To reduce the cost of experiments, many researchers tested small-scale models.

The majority of previous research using scale down modeling was focused on the shear mechanism, such as Sheikh & Toklucu (1993) [1], Park & Paulay (1975) [2] and Kani (1996) [3]. Up to authors' knowledge, no one has used SSM

* Corresponding author: ahmedyoussef@cu.edu.eg

 <http://dx.doi.org/10.28991/CEJ-2022-08-11-019>



© 2022 by the authors. Licensee C.E.J, Tehran, Iran. This article is an open access article distributed under the terms and conditions of the Creative Commons Attribution (CC-BY) license (<http://creativecommons.org/licenses/by/4.0/>).

to investigate the torsion mechanism. In this study, the torsional mechanism of one-eighth test miniature beams is investigated experimentally using two configurations of transverse RFT: In RC beams, rectangular staggered spiral stirrups are currently used as transverse RFT. The ductility, confinement, and continuity of these transverse configuration types are responsible for their newfound popularity. The benefit of using staggered spiral stirrups has been highlighted because the spiral continuity can boost structural member confinement and energy dissipation. Improving the torsional capacity of RC beams while preserving suitable economic and effective cross-sections presents a realistic challenge in our design. As a result, constructing and testing economically viable reinforcing methods for boosting the torsional capacity of RC beams is an essential part. The staggered spiral stirrup is one of these techniques that has shown exciting results in increasing the torsional capacity [4, 5].

Al-Zaidaneen et al. (2022) examined experimentally the shear performance, light-weight concrete beams reinforced with rectangular spiral hooks rather than ordinary hooks. The outcomes have revealed that implementing spiral hooks has boosted the shear capacity and deflection. Shear strength improvement has fluctuated from 3% to 47% when compared to the ordinarily hooked [6]. MohamedSalih & Yousif (2022), investigated the performance of (HSC) hollow beam reinforced with basalt fiber polymer (BFP) bars and steel hooks in combined shear, torsion, and moment. The variables were the proportion of longitudinal to transverse RFT, the diameter of BFP bars, and the steel hook spacing. The best results were obtained when beams with BFP bars and steel hooks with smaller diameters were used at closer spacings. The effect of longitudinal BFP bars generated better findings than steel hooks [7]. Ibrahim et al. (2022) analyzed the numerical and experimental search for hollow beams with spiral hooks as transverse RFT under torsion. An analysis using ANSYS software was performed to highlight the inclined spiral hook effect with diverse inclination angles and pitches on the torsional strength. A numerical equation had also been created to estimate the torsional capacity of these kinds of beams. Furthermore, the comparison of numerical and experimental outcomes was highly satisfactory, and the recommended equation strongly corresponds with both experimental and numerical results [8].

Hussain et al. (2022), investigated the fibres performance by examining twelve HSC beams under torsion load. Various parameters, such as diverse compressive strengths and fiber volume fractions with changeable transverse RFT spacing, were tested experimentally. When the fiber fractional volume is increased to 0.75, the maximum torque increases by about 27.1%. The outcomes show that as compressive strength increases, so does ultimate torsional strength, and this percentage increase increases with increasing fiber volume fraction [9]. Haroon et al. (2021), utilized artificial neural networks (ANNs) to investigate the structures underlying an RC member's torsional attitudes. The ANN model was developed and confirmed against a published experimental record of 159 beams. The findings demonstrate that ANNs can accurately model the torsional behaviour of RC beams [10]. Fawzy et al. (2021), investigated the beams torsional behavior when subjected to external lateral pressure over their lengths [11]. Shatarat et al. (2020), investigated the torsional mechanism using unwelded and welded transverse RFT. Diverse transverse RFT patterns were implemented: separate, circular spiral, rectangular spiral, and advanced spiral shape. The results displayed that the specimens with continuous circular hooks proved the efficiency compared with ordinary hooks, which obtained the greatest improvement of peak torsion resistance [12]. Katkhuda et al. (2019), Studied the beams torsional mechanism using transverse RFT in diverse shape: separate, continuous circular and rectangular spiral, and advanced rectangular spiral shape. The results showed that the applying of continuous rectangular spiral boosted the torsional resistance of 17% greater than applying separate reinforcements [13].

Ibrahim et al. (2020), investigated the contribution of spiral stirrups on boosting the beam torsional strength. Continuous spiral stirrups with an inclination angle and a monitorial pitch were tested for solid and hollow beams. The outcomes showed that the torsional strength of inclined spiral rectangular stirrups in solid and hollow beams increased by 16% and 18%, respectively. Furthermore, the outcomes showed that applying spiral ties resulted in more ductile failures and higher torsional angles [14]. Joh et al. (2019), conducted a pure torsion test on RC beams investigate a higher strength for steel and concrete manufactured from 80 MPa. The test variables were the longitudinal to transverse RFT ratio, the minimum torsional RFT ratio, and the total RFT ratio. They concluded that applying the minimum torsional RFT ratio approved by Eurocode 2 might give sufficient deformability under displacement-controlled mode to permit for torsional moment redistribution [15]. Rashidi et al. (2017), studied the contribution of longitudinal and transverse RFT on torsion strength, as well as the impact of reinforcement form on torsion strength. Ductility was found to rise with increasing reinforcement ratio. It was observed that longitudinal or transverse bars solely are not able to boost the torsional strength of RC beams, and both are required for good torsional behavior in RC beams [16]. Abdel-Kareem et al. (2020), examined beams with web openings for torsion test. Fifteen beams were examined: one solid with no opening, six without reinforcement all-round the opening, and eight with reinforcement created around the opening. The outcomes showed that applying inclined stirrups at a 45° angle to the samples' longitudinal pivot led to increase extreme torque till 90% from solid sample [17].

Staggered spiral stirrups are currently being used as transverse reinforcement in RC beams rather than closed ones. This newfound popularity can be attributed to the ductility, confinement, and continuity of these transverse configuration

types. The advantage of adopting staggered spiral stirrups has been highlighted because of the spiral continuity can boost the concrete confinement of the structural members and ductility [18-20] for all models, the torque was applied to lock the spirals. Improving the torsional capacity of RC beams whereas preserving suitable economic and effective cross-sections presents a realistic challenge in our design. As a result, constructing and testing economically viable reinforcing methods for boosting the torsional capacity of RC beams is an essential part. The staggered spiral tie is one of these techniques that has shown exciting results in increasing the torsional capacity [21-24]. The experimental torsional capacity values were compared to torsion strength values given by the ACI 318–14 [26] code and Eurocode-2 [27].

2. Research Significance

This study purposes to investigate the torsional failure mechanism of small-scale beams reinforced with an internally staggered continuous rectangular spiral. The experimental scheme comprises twelve rectangular-section one-eighth scale beams. Six beams were reinforced with closed stirrups while the other six were reinforced with staggered spiral stirrups as internal transverse reinforcement. The studied structural parameters were: (1) Stirrup's arrangement (closed stirrups– staggered spiral stirrups) and (2) The stirrups spacing (20-30-4-50-60-80 mm). All samples had identical reinforcement and concrete strength. The dimensions of the specimen's model (800×75×50 mm), which is equivalent to the dimensions of a prototype (6400×400×600 mm). The study was carried out using the small-scale model which was comprehensively emphasized in the literature and was partially confirmed for torsion problems in the current study. This research adopted an experimental investigation to examine the torsional behavior of RC beams miniatures with transverse RFT beneath diverse arrangement. Closed stirrups and rectangular staggered continuous spiral were used as transverse torsion RFT. The goal of this work was to assess the efficacy of spiral as internal torsion transverse reinforcement. Torsional moment-twist angle curves, load-mid span displacement curves, failure modes, and crack patterns were evaluated.

3. Experimental Program

3.1. Test setup

Test samples were tested in Concrete Research Laboratory, Cairo University. Load is applied to a diagonally spreader beam that distribute the load among two 0.15 m cantilevers through spherical seating as shown in Figure 1. A 25 kN load cell is used to measure the applied load. Figure 2 depicts the internal forces of the test sample. Through the use of two special sliding supports, the sample could rotate around its long axis. Two LVDTs (linear variable displacement transducers) have been used to calculate the rotation angle using vertical displacement and the cantilever length. A computer-controlled measurement system registers the LVDT measurements. Propagation of cracks, the failure mode, crack angle, and incremental loads were all realized during the test. Samples were loaded gradually till failure.



Figure 1. The set-up

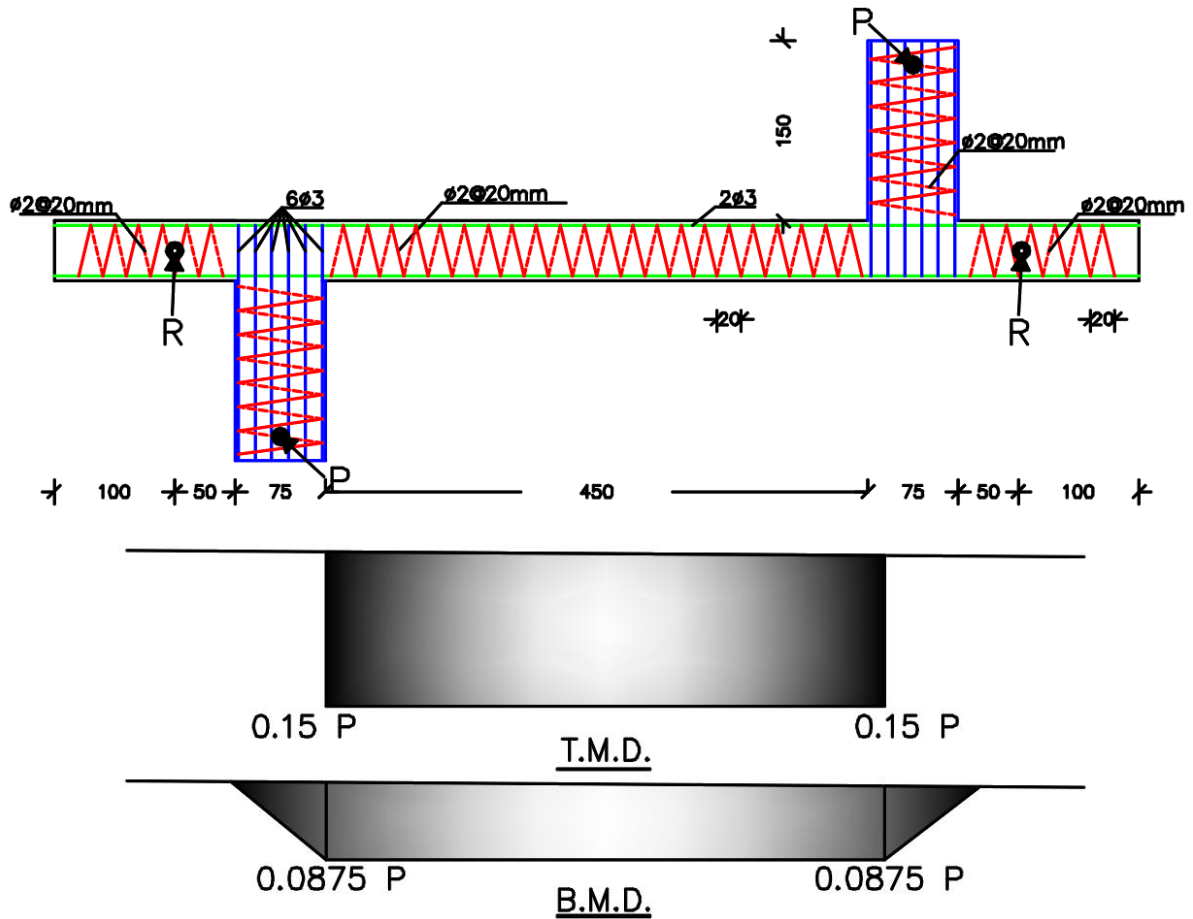


Figure 2. The miniature’s internal forces

3.2. Materials Properties

3.2.1. Mixture Characteristic

Mortar with a heterogeneous blend of sand, Portland cement, and water was used in construction. First cement and sand were dry mixed, and water is thereafter incorporated into this dry mix. The mixing ratio for water, cement, and sand is 0.42: 1.0:1.23. The samples are compacted using a mechanical vibrator. The samples were cured for 28 days in a water tank before being smoothed with fine sandpaper to reveal any cracks. Figure 3 depicts fine aggregate grading. For every beam, three cubes were casted to monitor the concrete compressive strength. After 28 days of curing, the sample’s compressive strength reached 40 MPa. To track the progress of cracks during testing, the samples were painted from the sides by white colour.

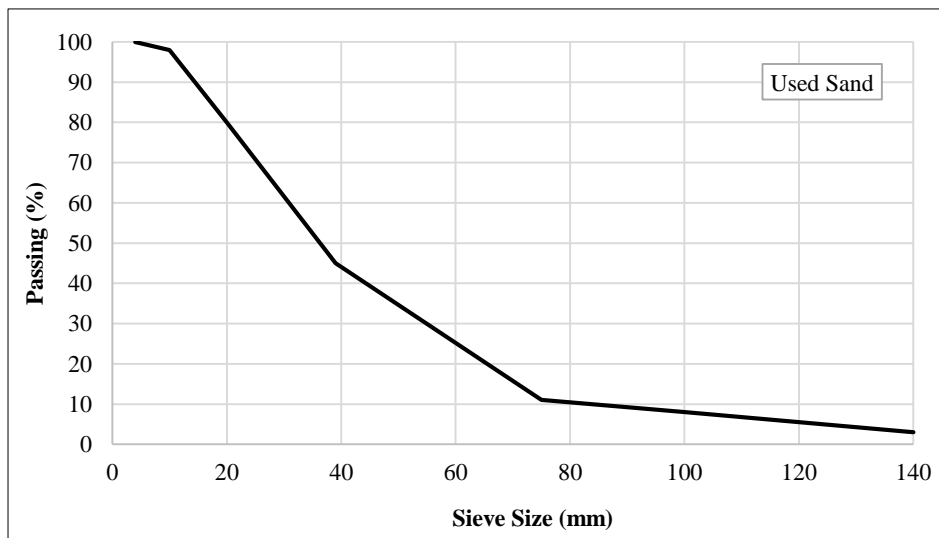


Figure 3. Fine aggregate grading

3.2.2. Reinforcement

High Strength smooth bars with diameters of 4mm and 3mm have been used as tensile and compressive RFT, respectively, and stirrups with diameters of 2 mm have been used. A standard tensile test was performed on three samples of each bar to evaluate the mechanical properties of the bars. The yield stress (F_y) of 4, 3, and 2 mm bars was found to be 690, 744, and 800 N/mm^2 , respectively. Figure 4 depicts the stress-strain curve for the bars with diameter of 4 mm. All samples were manufactured to have the same longitudinal and secondary reinforcement characteristic, as shown in Figure 5. The two cantilevers were reinforced with six 3 mm bars at the top and bottom, as well as transverse spiral stirrups with a diameter of 2 mm and a spacing of 30 mm. All samples had two top bars 3 mm and five bottom bars 4mm in longitudinal direction, but they had different transverse reinforcement arrangements within the torsional span: (1) six samples with closed stirrups (2) six samples with a continuous spiral rectangular shape.

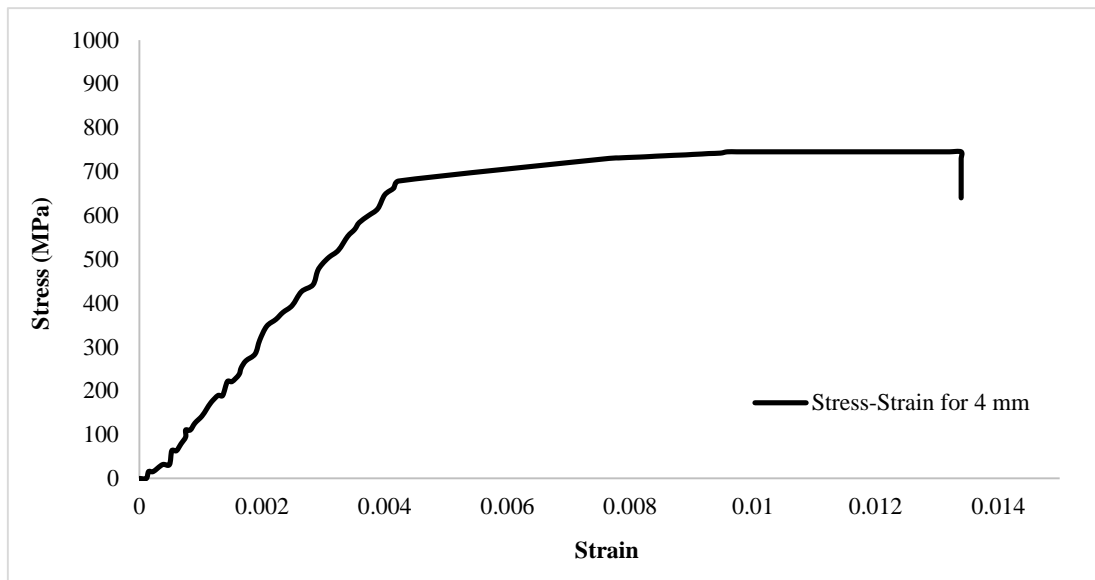


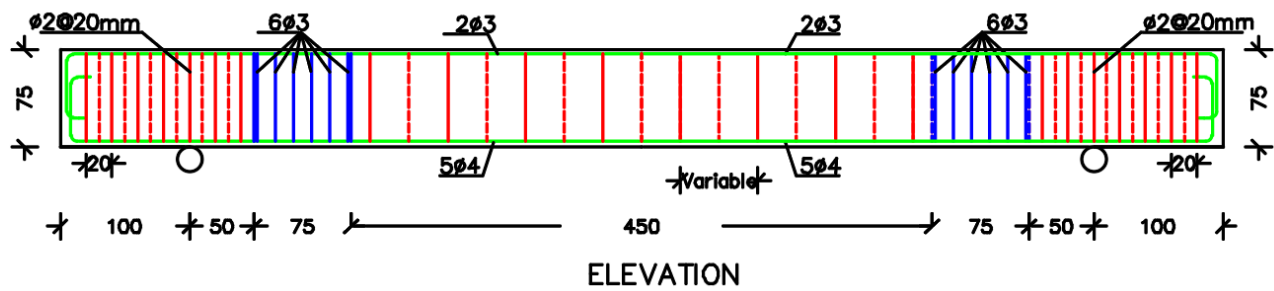
Figure 4. The stress-strain for the diameter bar of 4 mm



Figure 5. The sample's RFT

3.3. Details of Miniatures

A continuous staggered spiral stirrups spaced at six diverse intervals was used to reinforce six samples in transverse direction. Furthermore, closed stirrups, spaced at six different intervals was used to reinforce six samples in transverse direction. The samples' length was 900 mm, width was 50 mm, and depth was 75 mm. The cantilever length, width and depth were 150, 75, and 75 mm, respectively. The length of the examined region was 450 mm. To oblige the failure in the examined zone to be torsion-dominated, the terminal region of 150 mm length at each end of the sample was appropriately reinforced in transverse reinforcement with a large volume of spiral stirrups with 2 mm diameter spaced at 20 mm. The cantilevers were also heavily reinforced in order to avoid failure during the test. Figure 6 depicts the test sample dimensions and RFT details comprising six specimens of diverse stirrups spacing of 20, 30, 40, 50, 60, and 80mm. Table 1 shows a summary of reinforcement of test samples.



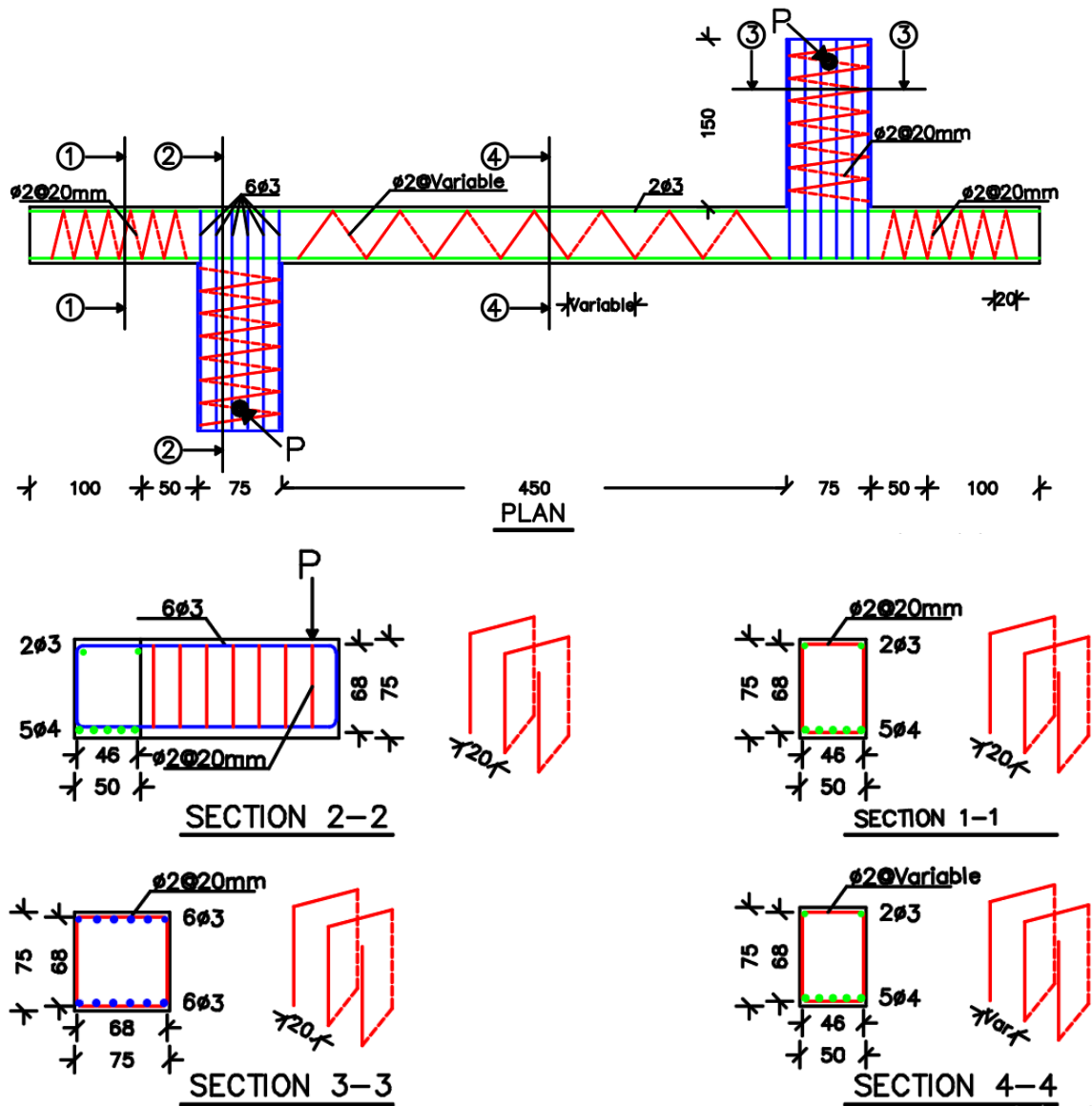


Figure 6. Test samples' dimension and reinforcement details

Table 1. Mechanical properties of the bars

Bar Diameter (mm)	Evaluated Area (mm ²)	Yield stress (MPa)	Tensile Stress (MPa)
4.0	12.60	690	766
3.0	7.10	800	868
2.0	3.14	744	828

4. Experimental Results and Discussions

4.1. Torsional Moment and Twist Angle

Figures 7 and 8 illustrate the effect of the stirrup spacing on the torsional moment and twist angle of the beams. The torsion capacity increased as the stirrup spacing decreased, as could be seen. The results show that the rectangular spiral RFT has a major effect on the torsion capacity of the sample beam. Torsion strength was higher in spirally samples than in closed stirrups samples. When the spacing was reduced from 80 to 20 mm, the peak torsional moment improved by around 220%. Using outcomes of the test as the deflections and load, the equivalent twist angle and torsion moment was plotted. For stirrup spacing of 20 mm, the sample revealed the highest load carrying capacity among all samples reinforced with spiral stirrups. Samples reinforced with spiral stirrups perform noticeably better than those reinforced with closed stirrups. It is noticed that the torsional moment-twist angle curves were separated into two areas. Firstly, the curves are linear till start cracking torsion. Secondly, the curves are nonlinear and the rotation angle extended quickly with increasing the torsional moment showing the post-cracking performance. The torsional moment and twist angle for spacing (20, 30, 40, 50, 60, and 80 mm) between spiral stirrups relating to closed stirrups are shown in Figure from 9 to 14.

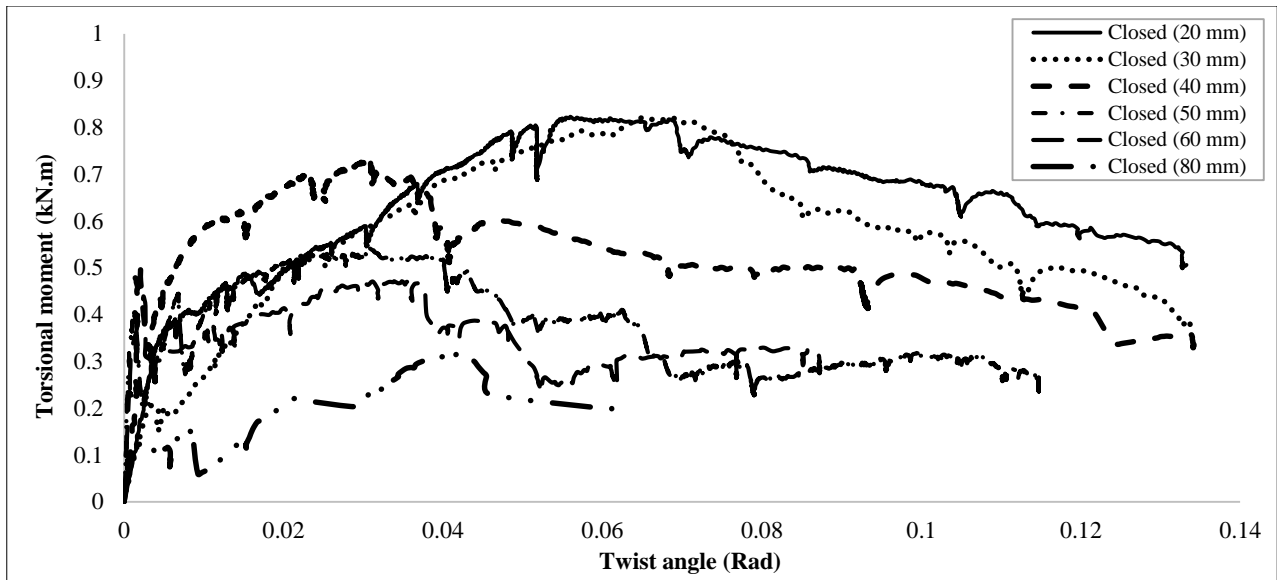


Figure 7. The torsional moment and twist angle of closed stirrups with changed spacing

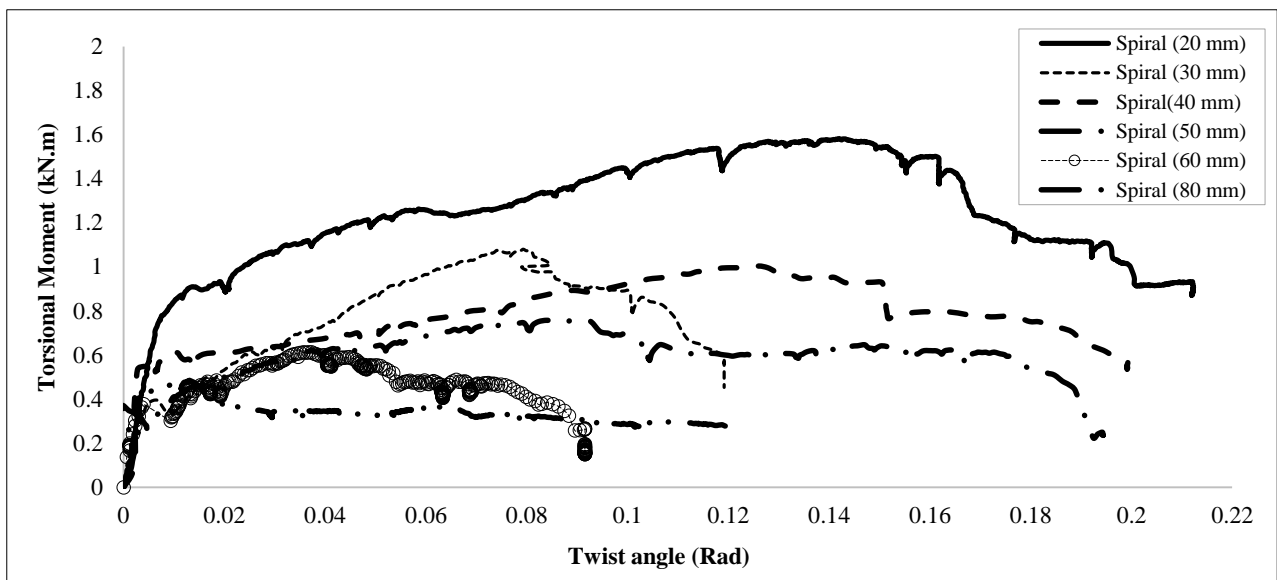


Figure 8. The torsional moment and twist angle of Spiral stirrup with changed spacing

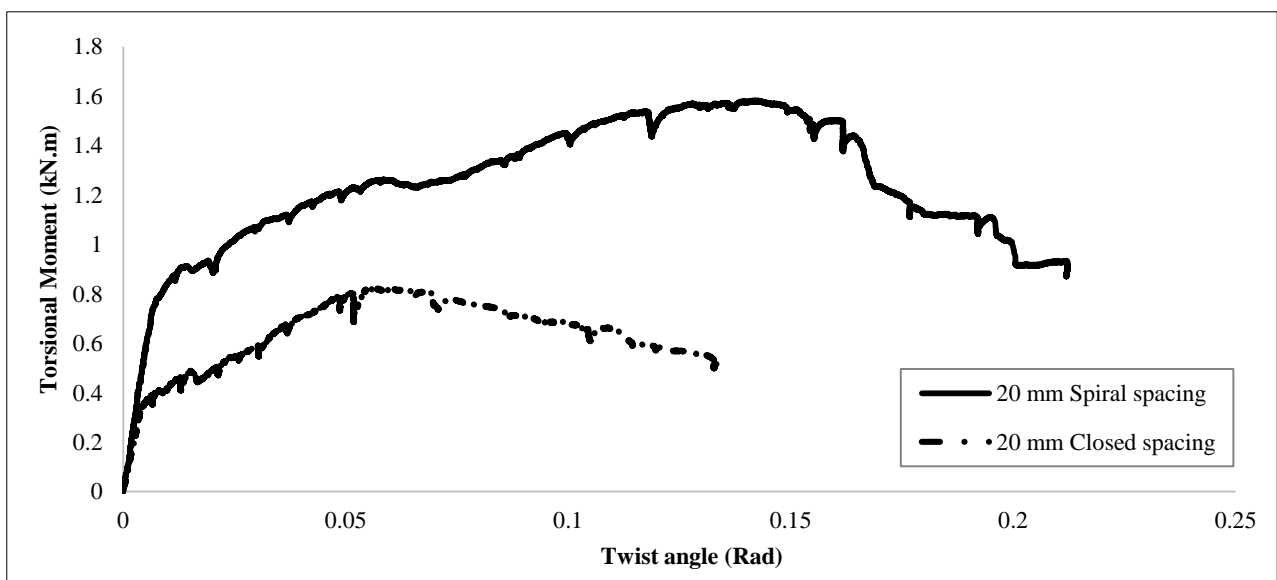


Figure 9. The torsional moment and twist angle of spiral and closed stirrup for spacing 20 mm

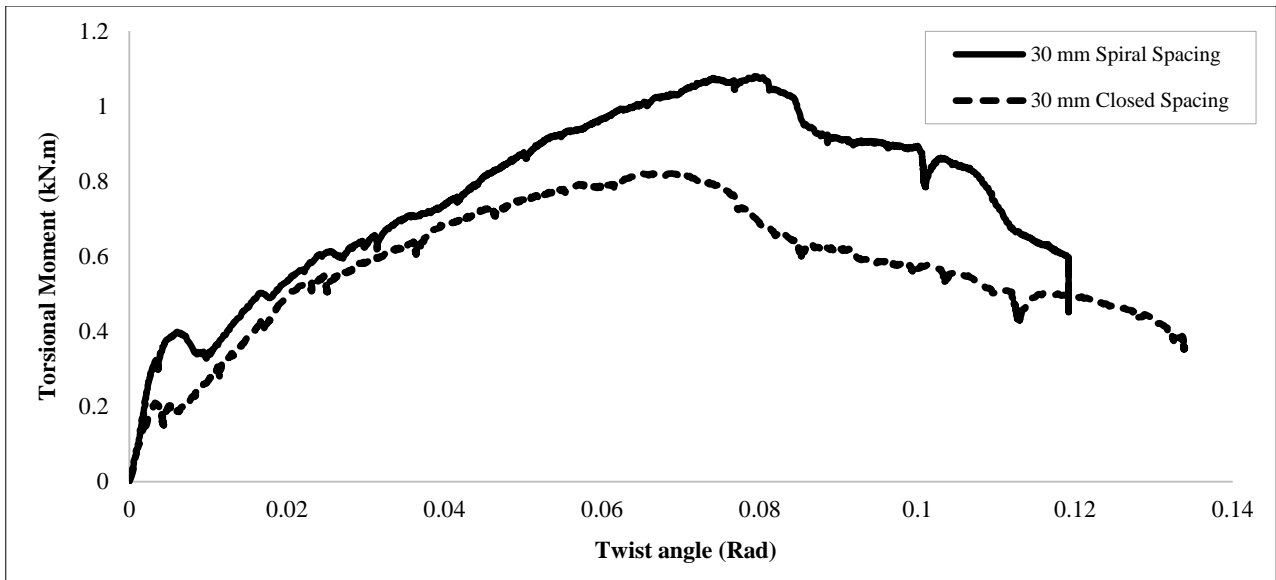


Figure 10. The torsional moment and twist angle of spiral and closed stirrup for spacing 30 mm

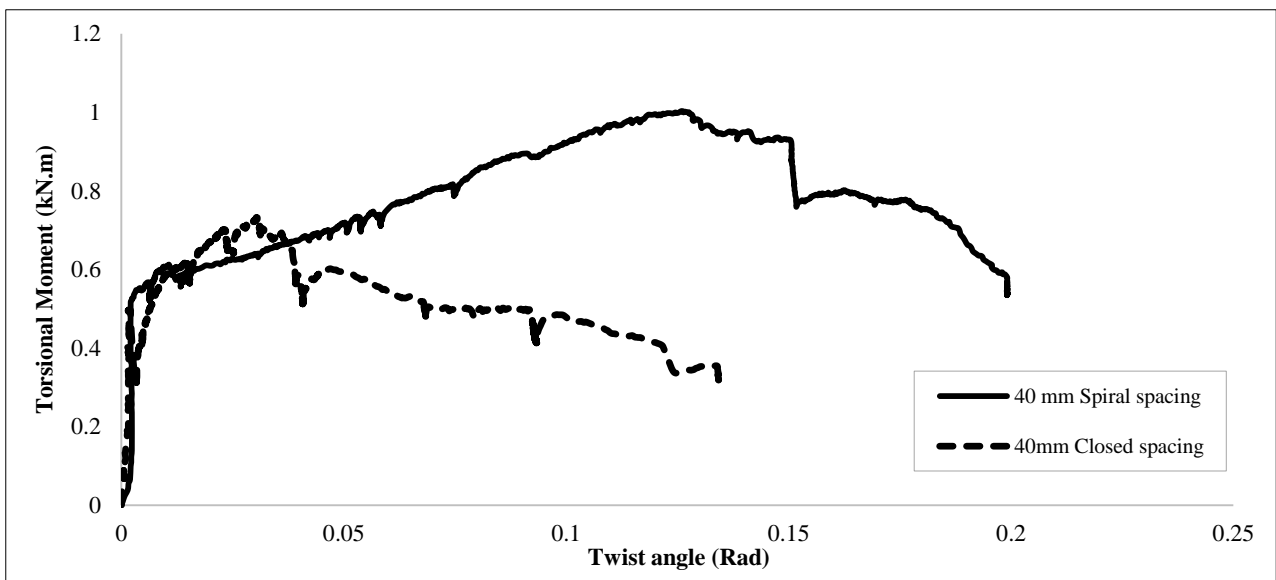


Figure 11. The torsional moment and twist angle of spiral and closed stirrup for spacing 40 mm

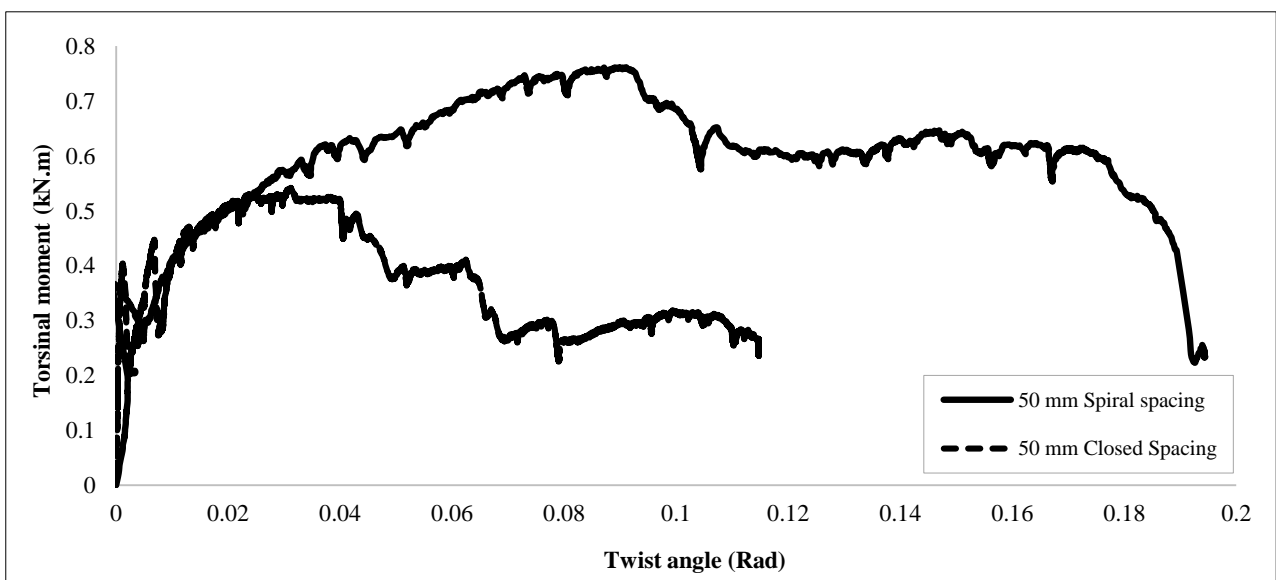


Figure 12. The torsional moment and twist angle of spiral and closed stirrup for spacing 50 mm

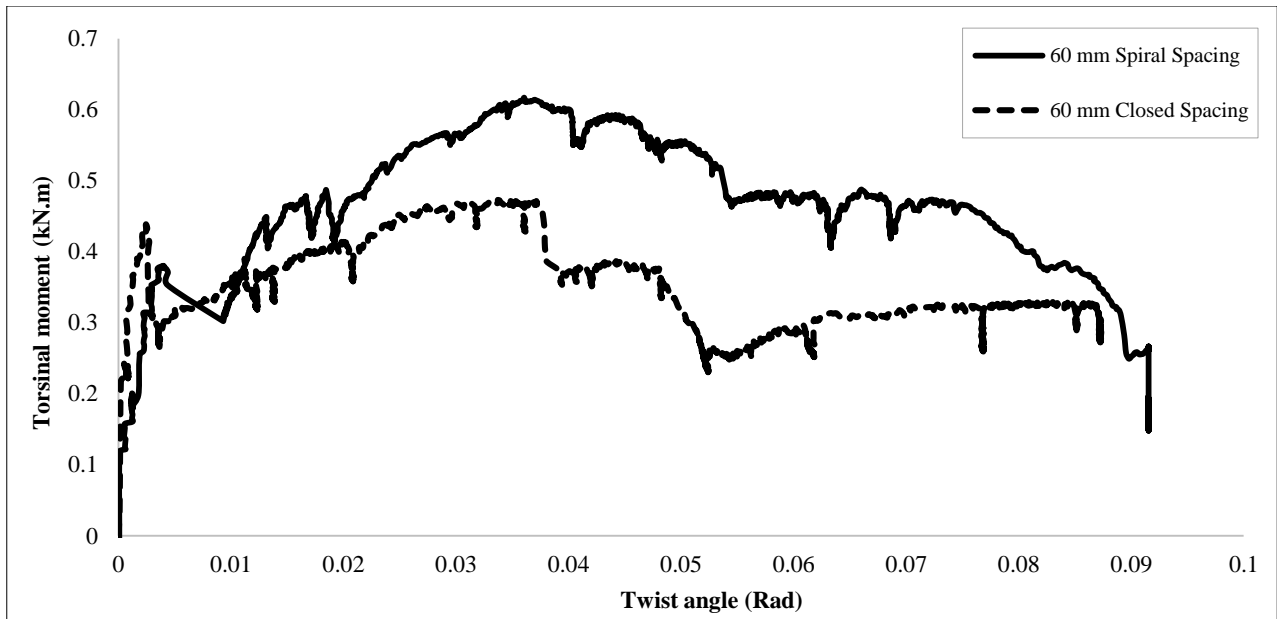


Figure 13. The torsional moment and twist angle of spiral and closed stirrup for spacing 60 mm

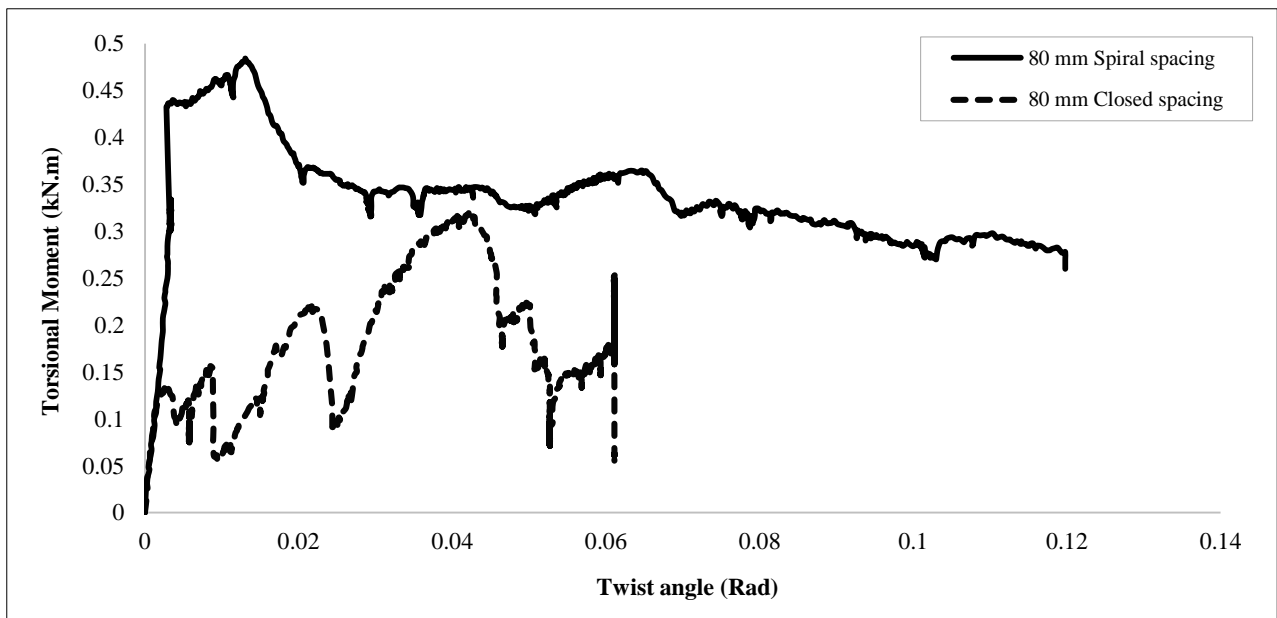


Figure 14. The torsional moment and twist angle of spiral and closed stirrup for spacing 80 mm

4.2. Cracking Pattern

4.2.1. Cracking for Closed Stirrups

Figures from 15 to 20 show the crack patterns of the samples reinforced with closed stirrups. Figure 15 shows the cracking pattern using closed stirrups for stirrup spacing $S=20$ mm. It can be seen from these images that closer the stirrup spacing lead to more the helical crack zone, and it allows for another crack to form. Helical oblique cracks are observed in all miniatures. As the distance between the stirrup increases, the helical main crack expands e.g. (localized helical crack). Torsional moment increases as stirrup spacing decreases. This may be explained that the smaller the stirrup spacing, the more efficacy because of covering a great circumference of the inclined cracks. In other words, a more efficient distribution of stirrups controls the cracks.



Figure 15. Crack pattern of closed stirrups for spacing 20 mm



Figure 16. Crack pattern of closed stirrups for spacing 30 mm



Figure 17. Crack pattern of closed stirrups for spacing 40 mm



Figure 18. Crack pattern of closed stirrups for spacing 50 mm



Figure 19. Crack pattern of closed stirrups for spacing 60 mm



Figure 20. Crack pattern of closed stirrups for spacing 80 mm

4.2.2. Cracking for Staggered Spiral Stirrups

Figures from 21 to 26 show the crack patterns of the samples reinforced with staggered spiral stirrups. Spiral stirrups beams retarded the cracking load, increased both the peak torsional strength and the twist angle. It was monitored that all samples pursued a similar failure mode. Helical oblique cracks were observed in all samples. The confinement effect of the spiral stirrups caused stress redistribution of the concrete. For stirrup spacing of 20 mm, the sample reinforced with spiral stirrups, at load of 6 kN, Hairline cracks were demonstrated. As the load increased, the cracks propagated where the crack sound was noticeable at a load of 10 kN. The sample was fully twisted at a load of 10.55 kN and a torsional moment of 1.55 kN.m. Torsional shear failure was indicated by a chain of helical crack pattern. Cracks were observed on the top surface and sides of the sample, forming a helical shape with 45-60 angle with the long direction. Although the two miniatures had the same amount of transverse torsion reinforcement ratio, the sample reinforced with spiral stirrups exhibited higher performance than the sample reinforced with closed stirrups.

Torsional moment and angle of twist were distinguished to determine the differences for all samples reinforced with spiral and closed stirrups. Continuous spiral stirrups had effect on retarding crack expansion. The deformation behavior of all samples was almost the same in the initial loading phase till the twist angle of 0.002667 rad/m, and then progressively enlarged till failure. The twist angle of the beam with spiral stirrups was less than that of twist angle of the closed stirrups under the same load level. The failure angles were evaluated from the sample beam side, where the orientation angle varied from 30 to 60. In addition, the loading configuration was able to retain the stiffness, preserve the flexure mode and promote the design safety for combined loaded beams submitted to combined torsional moments, bending moments and shear forces. This can be described that the closer the stirrups interval, the more efficacious closing the helical cracks.



Figure 21. Crack pattern of spiral stirrups for spacing 20 mm



Figure 22. Crack pattern of spiral stirrups for spacing 30 mm



Figure 23. Crack pattern of spiral stirrups for spacing 40 mm



Figure 24. Crack pattern of spiral stirrups for spacing 50 mm



Figure 25. Crack pattern of spiral stirrups for spacing 60 mm



Figure 26. Crack pattern of spiral stirrups for spacing 80 mm

4.3. Effect of Transverse Reinforcement Interval

This section illustrates the influence of transverse torsion reinforcement interval arrangement on the torsional performance of specimens. Two stirrup arrangements have been used: closed stirrups and continuous staggered spiral stirrups. For transverse RFT, six spacing (20, 30, 40, 50, 60, 80 mm) were properly considered for every stirrup's arrangement. The samples made with continuous spiral stirrups attain the greatest boost in the peak torsional capacity. Furthermore, the peak torsional capacity development proportion in correlation to the closed arrangement is acquired with 20 mm arranged stirrups (87%), pursued by 30 mm arranged stirrups (54%). Because the spiral arrangement is continued, it can improve the samples' resistance capacity when submitted to torsional moments. It is demonstrated that increasing the number of stirrups provided by decreasing the stirrups interval, results a significant increase in the torsional capacity of test specimens. Table 2 outlines the peak torsion moment, dissipated energy, and displacement at peak load for each value of spacing stirrup for closed and spiral stirrups. Figure 27 depicts the relationship of the peak torsion Moment and the stirrup spacing for closed stirrups. Figure 28 depicts the relationship between the peak torsion moment and the stirrup spacing for spiral stirrups. It is deduced that the torsional moment increases as stirrup spacing decreases. For spacing 20 mm, the highest torsion Moment was achieved for staggered spiral stirrups. Figure 29 depicts the relationship between displacement at peak load and stirrup spacing for closed stirrups. Figure 30 depicts the relationship between displacement at peak load and stirrup spacing for spiral stirrups. The same trend is seen with increased deformability at peak load as stirrup spacing is reduced.

Table 2. Test results for samples with diverse stirrups spacing for closed and spiral stirrups

Model	Stirrup spacing (mm)	Peak Torsion Moment (kN.m)	Displacement at peak load(mm)	Dissipated energy (kN.m)
BC1	20	0.82	10.05	51.69
BC2	30	0.80	8.52	50.2
BC3	40	0.732	6.04	40.53
BC4	50	0.54	5.475	34.16
BC5	60	0.32	5.25	27.5
BC6	80	0.31	4.725	11.23
BS1	20	1.54	18.9	98.13
BS2	30	1.07	15	92
BS3	40	1.003	15	65.0115
BS4	50	0.751	13.7	44.017
BS5	60	0.616	9	35.6624
BS6	80	0.48	7.5	16.76

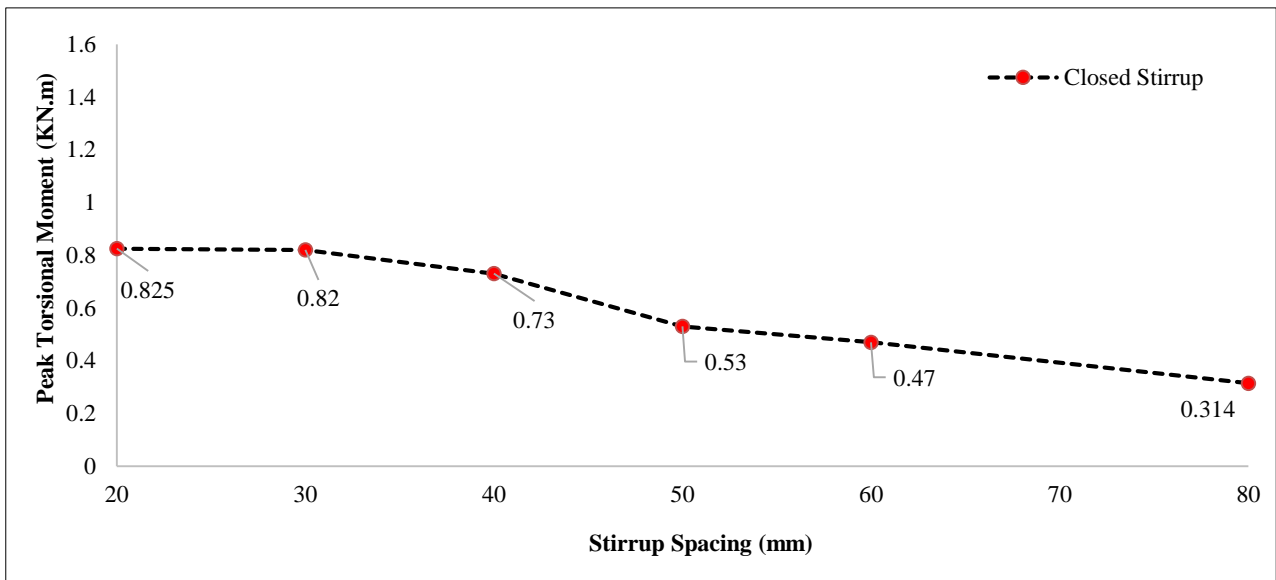


Figure 27. The relationship of the peak torsion Moment and the stirrup spacing for closed stirrups

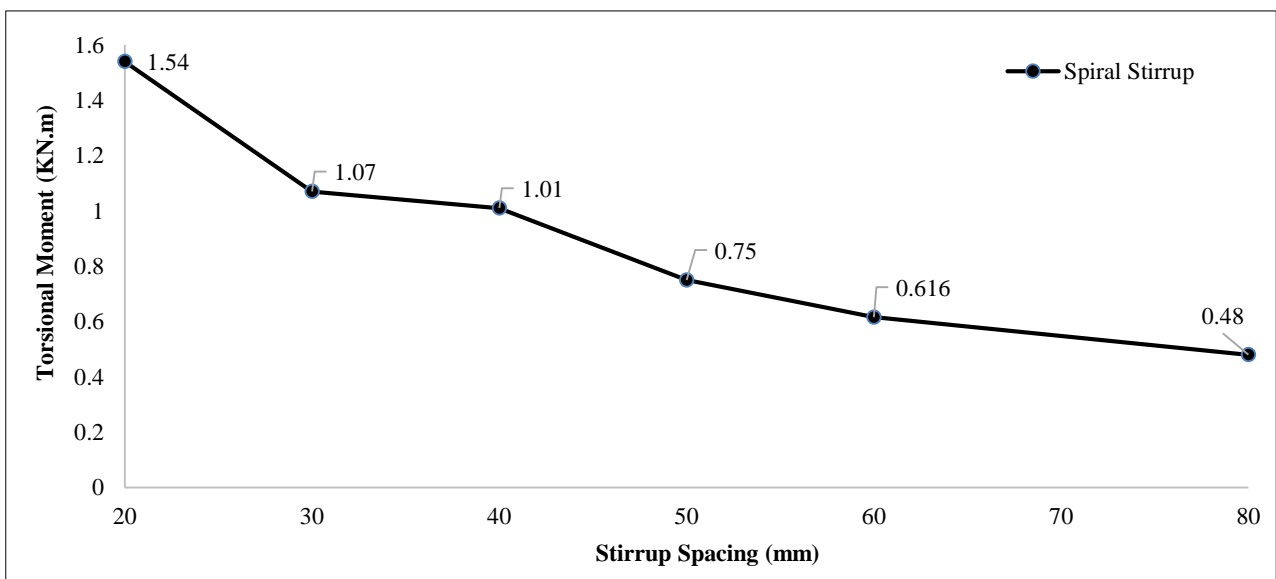


Figure 28. The relationship of the peak torsion Moment and the stirrup spacing for spiral stirrups

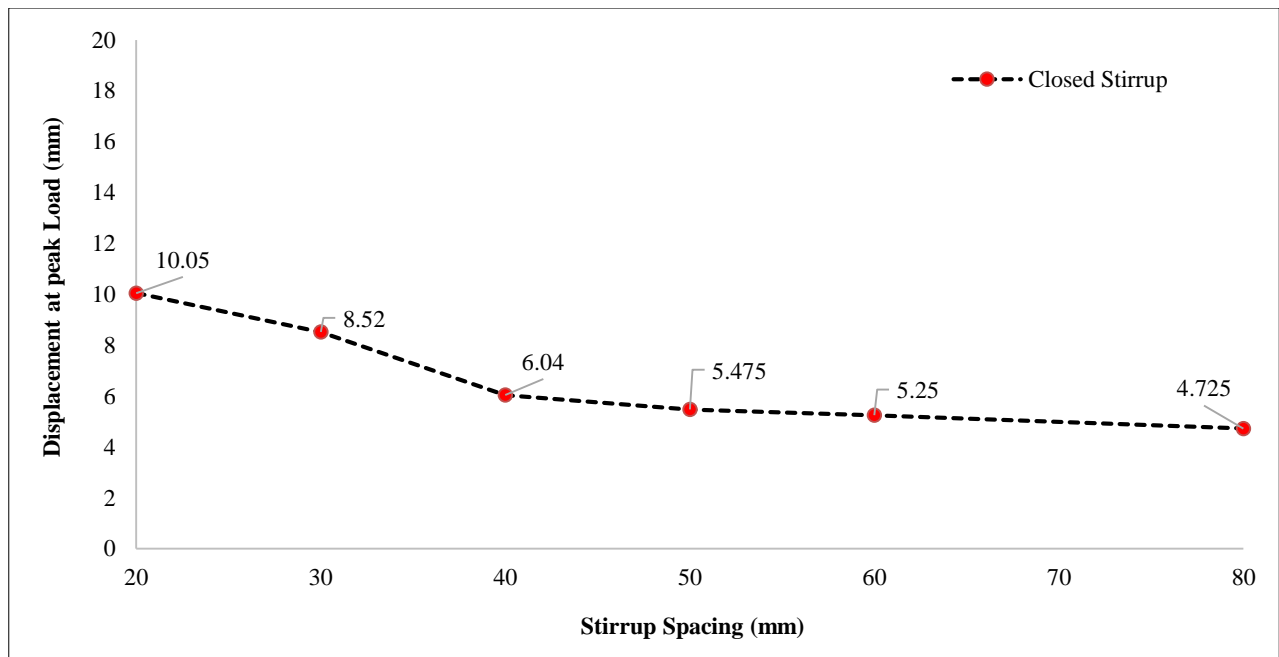


Figure 29. The relationship of the displacement at peak load and the stirrup spacing for closed stirrups

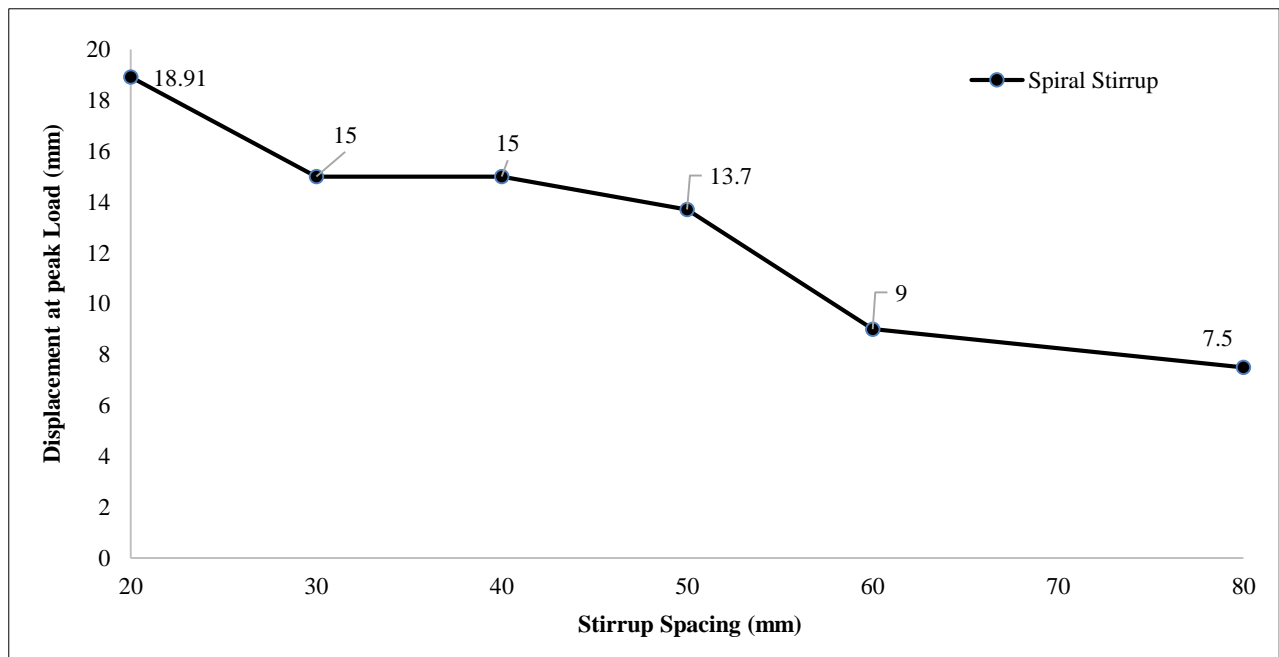


Figure 30. The relationship of the displacement at peak load and the stirrup spacing for spiral stirrups

4.4. Dissipated Energy

The area under the torsional moment –twist angle curve up to the failure load is used to calculate the dissipated energy. The dissipated energy for the miniatures enhanced with staggered spiral stirrups and proved the greatest dissipated energy compared to the other miniatures. When the stirrup spacing, S , is reduced, the dissipated frequency is increased. The results showed that the optimal dissipated energy was 98.13 kN.m at spiral stirrup spacing $S=20$ mm. Staggered spiral stirrups would be used to optimize the miniature's resistance to torsion. When the stirrup interval, S , was reduced, the deformations at peak load slightly increased, and thus the dissipated energy increased. Closer stirrup spacing firmly closed the helical cracks and caused large deformations when compared to larger stirrup spacing. Giving that both were able to retard the torsion failure, the smaller spacing might give better deformations. Figure 31 depicts the relationship between dissipated energy and stirrup spacing for closed stirrups. Figure 32 depicts the relationship between dissipated energy and stirrup spacing for spiral stirrups. It was discovered that the dissipated energy for the miniatures reinforced with closed stirrups was extremely high. When the stirrup spacing is reduced, the dissipated energy increases slightly.

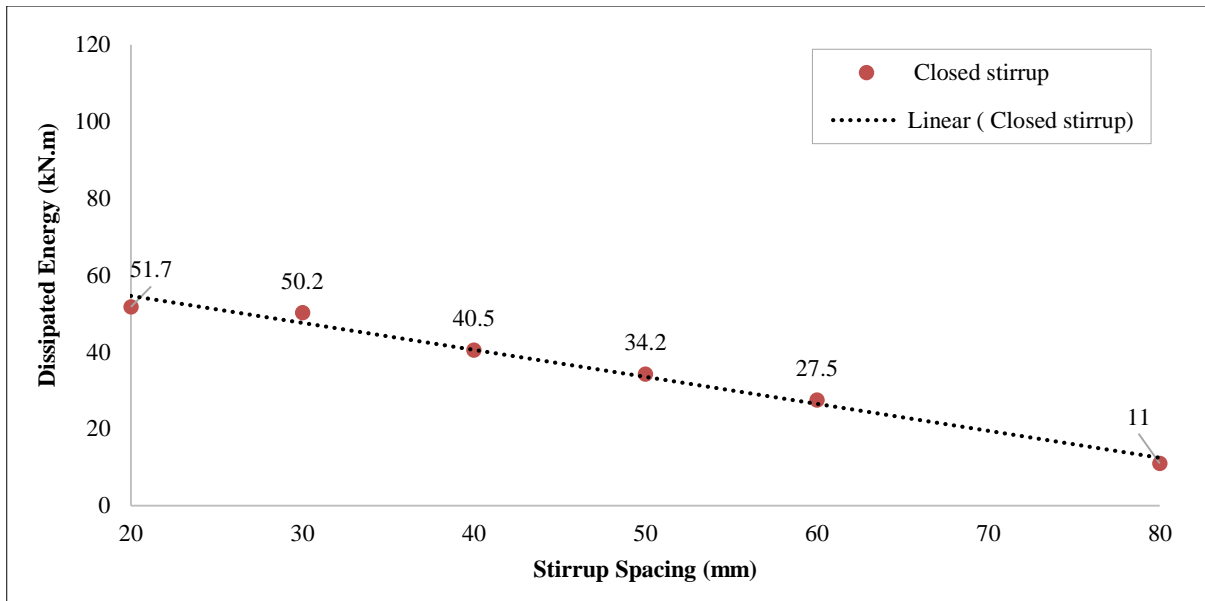


Figure 31. The relationship of the dissipated energy and the stirrup spacing for closed stirrups

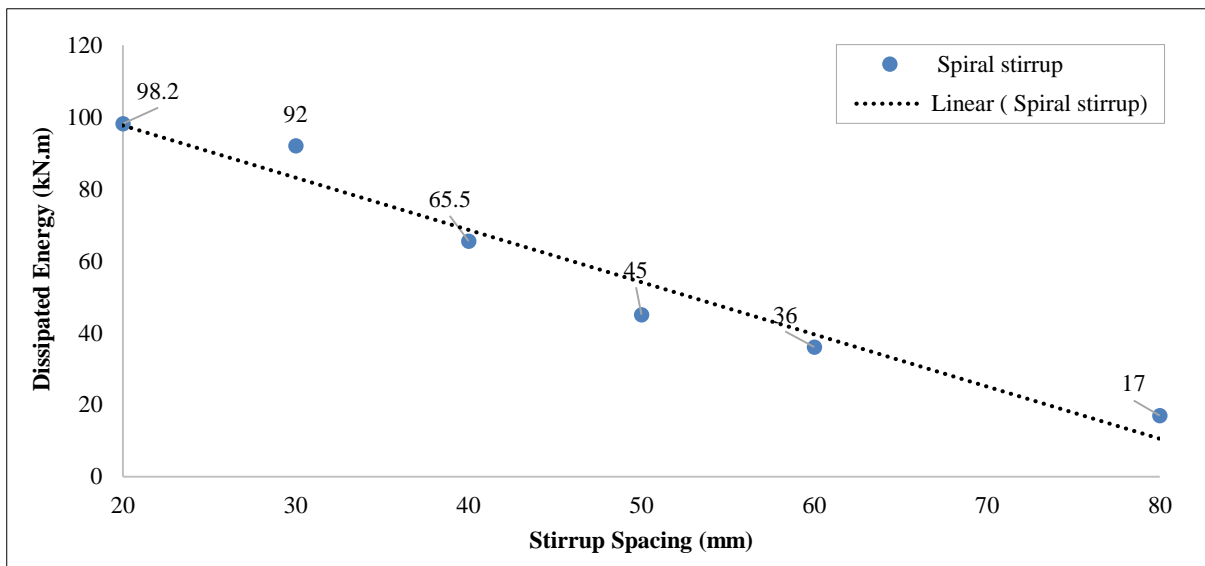


Figure 32. The relationship of the dissipated energy and the stirrup spacing for spiral stirrups

4.5. The Relationship Between the Small Scale and the Prototype

This is a critical section in the experimental scale down results are converted into full scale behaviour by correlating the data. Because the prototype and the model are linked, the small model's results will be interpreted to predict the behaviour of the prototype. The purpose of this research is to obtain full-scale design information by correlating data from small-scale model experiments. Furthermore, the relationship between the prototype and small scales is demonstrated. The steel's stress similitude has been preserved, whereas $f_{y\ model}$ is 690 MPa as opposed to $f_{y\ prototype}$ 400 MPa for the prototype. By using staggered continuous stirrups instead of closed stirrups, we can reduce the volume of stirrups while maintaining the same torsion capacity. The equivalent Prototype section is ($f_{y\ prototype}$ = 400 MPa), $B \times d=400 \times 600$ mm, Beam length=6400, Tensile reinforcement $4\phi 19$, Compressive reinforcement $2\phi 12$, stirrups $\phi=8$ mm, and $F_{cu}=40$ MPa. A comparison of the experimental peak strength of test miniatures using spiral stirrups and closed stirrups with diverse spacing between stirrups. Geometrical similitude has been preserved stress similitude for the steel as shown in Equation 1 [23]. Table 3 show test results for prototype with diverse stirrups spacing. Figure 33 shows torsional moment and stirrup spacing for prototype for spiral and closed stirrups. Figure 34 shows displacement at peak load and stirrup spacing for prototype for spiral and closed stirrups.

$$\frac{Moment_{prototype}}{Moment_{model}} = Scale^3 \frac{f_{y\ prototype}}{f_{y\ model}} \tag{1}$$

Table 3. Test Results for prototype with diverse stirrups spacing for closed and spiral stirrups

Model	Stirrup spacing (mm)	Peak Torsion Moment (kN.m)	Displacement at peak load(mm)
BC1	160	43.81	80
BC2	240	42.74	68
BC3	320	39.11	48
BC4	400	28.85	43.2
BC5	480	17.1	42
BC6	640	16.56	37.6
BS1	160	82.2	144
BS2	240	57.17	120
BS3	320	53.59	120
BS4	400	40.12	110
BS5	480	32.91	72
BS6	640	25.64	60

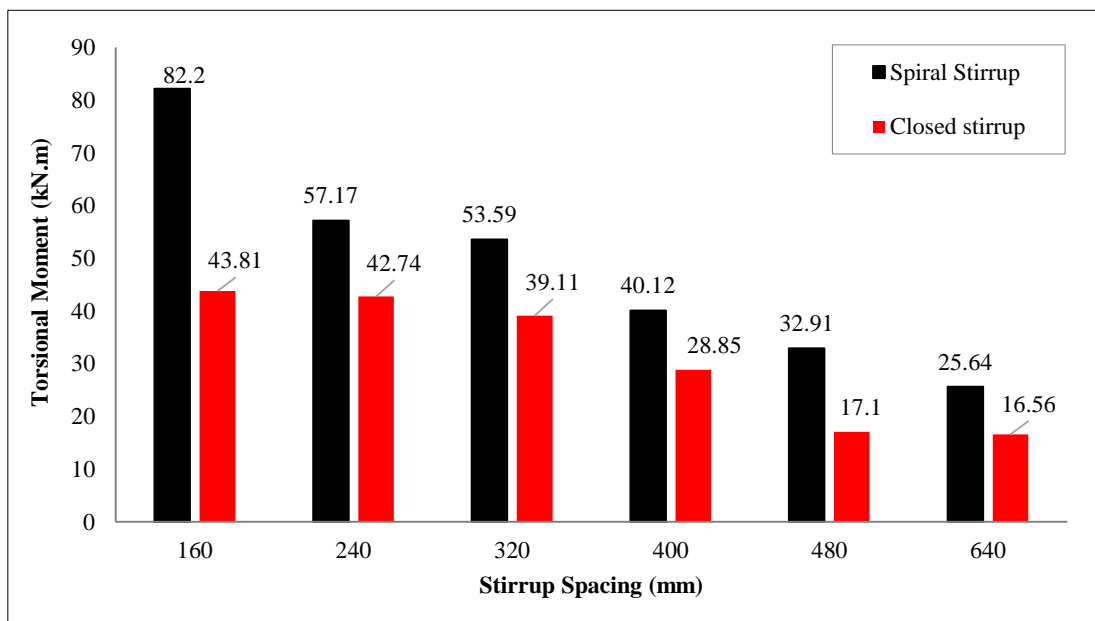


Figure 33. Torsional moment and stirrup spacing for prototype for spiral and closed stirrups

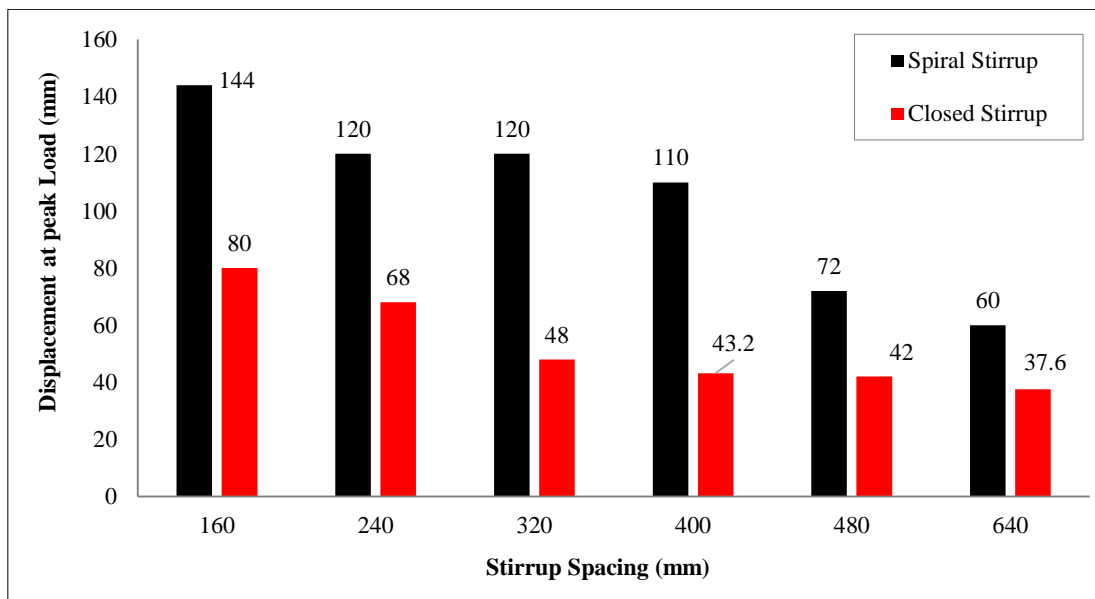


Figure 34. Displacement at peak load and stirrup spacing for prototype for spiral and closed stirrups

4.6. Comparison among Different Transverse RFT

To evaluate the efficacy of two techniques, the weight of RFT for every technique is assessed and compared in all studied cases. The most strength was acquired by using a spiral stirrup. It can be noted that the staggered spiral stirrup demonstrated the greatest strength and thus may be considered the most efficient RFT technique for shear of miniatures beams. Figure 35 shows the weight for each transverse RFT technique. The greatest weight was C1 for the miniature reinforced with closed stirrups and stirrups spacing 20 mm. It can be deduced that closed stirrups showed the highest weight and therefore requires more cost, and therefore it is preferable to use the spiral stirrups and hence it may be considered the most efficient Transverse technique.

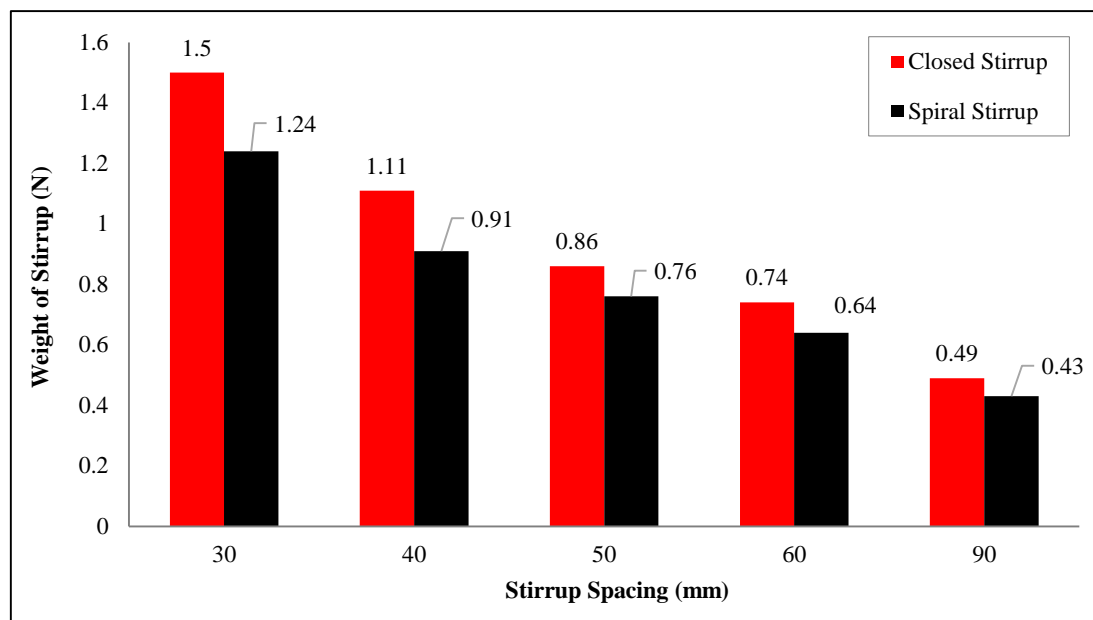


Figure 35. The weight for the miniatures strengthened with spiral and closed stirrups

5. Determining the Difference among Results and Design Codes (Analytical Background)

The torsional capacity for RC models is theoretically analyzed in this division. The expected moments are computed using the ACI Standard formulation [26], Eurocode-2 [27], Japan standard specification (JSCE-2007) [29], and Egyptian code [25].

5.1. Eurocode-2 [27]

The Eurocode-2 presents formulas for assessing the torsional capacity of beams with vertical hooks. Three distinctive formula have been created and the least magnitude will be chosen. The first magnitude is linked to the stirrup’s contribution to the torsional resistance. The second one magnitude is linked to the longitudinal contribution to the torsional resistance. Torsional capacity of the concrete struts is the third amount. The slightest of these three amounts is the torsional strength of the part. The torsional strength is the smallest of these three amounts. T_{Ed} denotes the applied design torsion in kN m, A_k : the area bounded by the connecting lines' center-lines. Z_i denotes the side length of beam, V_{Ed} : the design shear force in the section under consideration as a result of external loading and prestressing kN (unbonded), $V_{Rd,max}$: the peak shear force design value, which the member can sustain, but is limited by crushing kN of the compression struts, $V_{Rd,s}$ the design value of the shear force that can be applied kN is sustained by yielding shear reinforcement.

$$T_{u1} = f_{ys} \left(\frac{A_{sw}}{s} \right) 2 A_k \cot \theta_t \tag{2}$$

$$T_{u2} = f_y \left(\frac{A_s}{u_k} \right) 2 A_k \tan \theta_t \tag{3}$$

$$T_{u3} = 2 v f_c A_k \frac{A}{u} \sin \theta \cos \theta \tag{4}$$

$$V_{Rd,max} = \frac{(\alpha_{cw})(b_w)(z)(v_1)(f_{cd})}{(\cot \theta) + (\tan \theta)} \tag{5}$$

$$V_{Rd,s} = \frac{(A_{sw})(Z)(f_{ywd})(\cot \theta_t)}{s} \tag{6}$$

$$V_{Ed} = \tau_{t,i} t_{ef} Z_i \tag{7}$$

$$v = 0.6 \left(1 - \frac{f_c}{250}\right) \quad (8)$$

$$\tau_{t,i} = \frac{V_{Ed}}{t_{ef} Z_i} \quad (9)$$

5.2. ACI Standard [26]

According with ACI-318-14 code [26], the torsional capacity for RC beams prior to actually cracking is determined using the Equation:

$$T_{cr} = 0.33 \times \sqrt{f_c} c \left(\frac{A_{cp}^2}{P_{cp}}\right) \quad (10)$$

The ACI-318-14 [26] standard recommends the following formulas for determining the peak torsional capacity of RC beams.

$$T_{us1} = f_{yst} \left(\frac{A_{sw}}{s}\right) 2 A_o \cot \theta_t \quad (11)$$

$$T_{us2} = f_y \left(\frac{A_{sl}}{P_h}\right) 2 A_o \cot \theta_t \quad (12)$$

$$A_s = \left(\frac{f_{ys}}{f_y}\right) \left(\frac{A_{sw}}{s}\right) u_t \cot \theta_t^2 \quad (13)$$

where A_{st} is surface area of one-legged hooks (mm^2), f_{yst} : transverse RFT yield strength (MPa), s : interval between hooks (mm), A_{sl} : longitudinal RFT area (mm^2), f_y : longitudinal RFT yield strength (MPa), P_h : the perimeter of the hoops' central axis, mm, α : angle of cracks (degree), A_{cp} : the area bounded by the outside boundary of a cross section, P_{cp} : The outside boundary of a miniature cross section in mm, A_o the total area bounded by shear flow path, $A_o = 0.85 A_{oh}$, and A_{oh} area bounded by the stirrups central.

The theoretical peak torsional capacity is managed by the least magnitude of the above formulas. Moreover, the crack angle of inclination must've been between 30 and 60 to implement ACI equations. It must be remarked that the crack angle regarded to ACI equation is the angle measured during test. The two preceding formulas clearly ignored the concrete contribution after cracking and depended on transverse and longitudinal torsional resisting capacity.

5.3. Japan Standard Specification (JSCE -2007) [29]

The design capacity for diagonal compression failure of web concrete against torsion, M_{tcd} , may be obtained as shown in Equation 14. The design torsional capacity for rectangular cross sections, M_{tyd} as shown in Equation 15.

$$M_{tcd} = 1.25 \sqrt{f'_{cd}} / \gamma_b \quad (14)$$

$$M_{tyd} = 2 * A_m \sqrt{q_w q_l} / \gamma_b \quad (15)$$

$$q_w = A_{tw} f_{wd} / s \quad (16)$$

$$q_l = A_{tl} f_{ld} / U \quad (17)$$

5.4. Egyptian Code (EPC203-2020) [25]

The peak shear stress produced as a result of the peak torque is given by Equation 14. The torsional stresses do not exceed the $q_{u,min}$ given by Equation 14. The area of one tie stirrup branch A_{str} is given by Equation 14. Where X_1 and Y_1 are the smaller and greater center-to-center dimensions of closed stirrups, respectively. The diagonal force needed for the space truss model's equilibrium is carried by the concrete compression diagonal. Limiting both the concrete strut compressive stresses and the maximum shear stress avoided the crushing failure of the compression diagonal. The shear stress is limited by the ECP 203 to the value given by Equation 14. The longitudinal reinforcement area A_{sl} is offered by Equation 21. Figure 2 depicts the cross-sectional area of RC beam.

$$Q_{tu} = \frac{M_{tu}}{2 * A_o * t_e} \quad (18)$$

$$M_{tu} = \frac{1.7 * b_1 * t_1 * A_{str} * f_{yst}}{s} \quad (19)$$

$$Q_{tumin} = \frac{0.4 - b * s}{f_{yst}} \quad (20)$$

$$A_{sl} = \frac{A_{str} * p_h * f_{yst}}{s * f_y} \tag{21}$$

$$q_{tmin} = 0.06 \sqrt{\frac{f_{cu}}{\gamma_c}} \tag{22}$$

$$q_{tmax} = 0.7 \sqrt{\frac{f_{cu}}{\gamma_c}} \tag{23}$$

6. Comparison of Analytical and Experimental Results

Table 4 illustrates the comparison between prototype results and analysis predictions by ACI Standard formulation [26] and Eurocode-2 [27]. Table 5 illustrates the comparison between prototype results and analysis predictions by Japan standard specification (JSCE -2007 [29]) and EPC203-2020 [25].

Table 4. Comparison between prototype results and analysis predictions

Stirrup Spacing	Tu EXP		ACI318-14 [26]		Euro Code [27]	
	Tu	Tu, ACI	Tu,EXP / Tu,ACI	Tu, EC	Tu,EXP / Tu,EC	
160	43.81	30.8	1.42	40.95	1.07	
240	42.74	20.51	2.08	27.3	1.57	
320	39.11	15.38	2.54	20.5	1.91	
400	28.85	12.3	2.35	16.4	1.76	
480	17.1	10.25	1.67	13.7	1.25	
640	16.56	8.8	1.88	11.7	1.42	
160	82.2	30.8	2.67	40.95	2.01	
240	57.17	20.51	2.78	27.3	2.09	
320	53.59	15.38	3.48	20.5	2.62	
400	40.12	12.3	3.26	16.4	2.45	
480	32.91	10.25	3.21	13.7	2.40	
640	25.64	8.8	2.91	11.7	2.19	

Table 5. Comparison between prototype results and analysis predictions

Stirrup Spacing	Tu EXP		ECP2020		JSCE 15	
	Tu	Tu, ECP	Tu,EXP / Tu, ECP	Tu,JS	Tu,EXP / Tu,JS	
160	43.81	30.8	1.42	37.8	1.16	
240	42.74	20.51	2.08	30.71	1.39	
320	39.11	15.4	2.54	26.6	1.47	
400	28.85	12.3	2.35	23.8	1.21	
480	17.1	10.25	1.67	21.71	0.79	
640	16.56	8.9	1.86	18.8	0.88	
160	82.2	30.8	2.67	37.8	2.17	
240	57.17	20.51	2.79	30.71	1.86	
320	53.59	15.4	3.48	26.6	2.02	
400	40.12	12.3	3.26	23.8	1.69	
480	32.91	10.25	3.21	21.71	1.52	
640	25.64	8.9	2.88	18.8	1.36	

The expected moments are computed using the ACI Standard formulation [26], Eurocode-2 [27], Japan standard specification (JSCE -2007) [29], and Egyptian code [25]. The calculated and observed torsional moments of the test samples are described in Table 5. The anticipated results from the Euro-code and the ACI-318-14 formulation [26] are very close, as shown in Table 5. Based on these comparisons, it is clear that the Eurocode (EC2-04) [27] and the ACI Code (ACI 318-14 [26]) design requirements are conservative in forecasting the torsional moments of the beams within a good margin. As a result of these comparisons, it is easy to conclude that code design forecasting (Eurocode (EC2-04) [27] and ACI Building Code (ACI 318-14 [26]) implemented to the use of stirrups can also be utilized to spirally

reinforced beams with conservative results. The predictable torsional moment is in line with the experimental torsion, as shown in Table 5, whereas the experimental results are lightly larger than the analytical ones. As previously demonstrated by test specimen results, spiral staggered continuity has a significant influence on beams. Figure 36 displays JSCE [29], ACI [26], Euro [27], ECP [25], and experimental T_u for closed stirrups. Figure 37 displays JSCE [29], ACI [26], Euro [27], ECP [25], and experimental T_u for spiral stirrups.

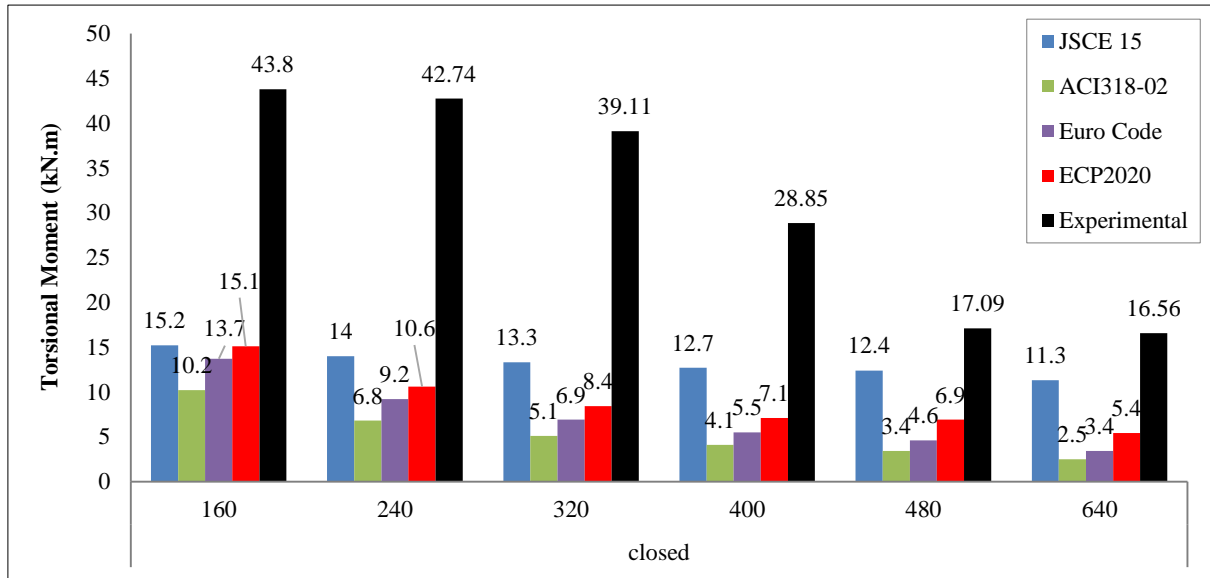


Figure 36. JSCE [29], ACI [26], Euro [27], ECP [25], and experimental T_u for closed stirrup

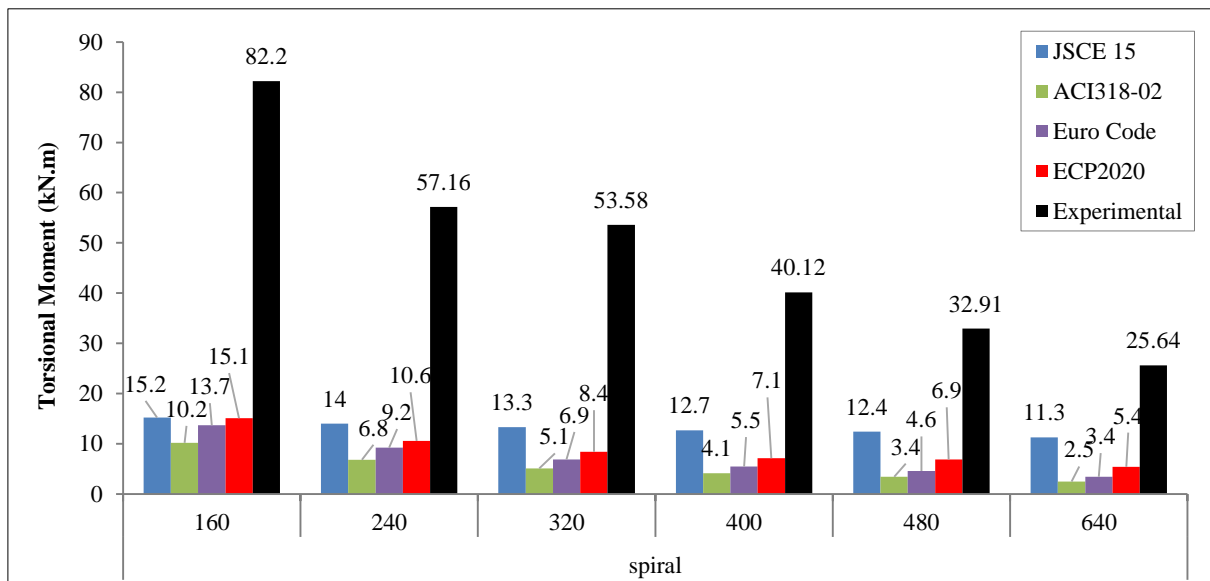


Figure 37. JSCE [29], ACI [26], Euro [27], ECP [25], and experimental T_u for Spiral stirrup

7. Conclusion

The current research adopted an experimental investigation to examine the torsional behavior of small-scale beams specimens with closed stirrups and rectangular continuous staggered spiral transverse torsion reinforcement. Twelve rectangular specimens with identical reinforcement detailing were loaded in torsion and tested until collapse. The goal of this work was to assess the efficacy of spirals as internal transverse reinforcement. The effect of staggered spiral stirrups on the behavior of reinforced mortar beams under torsion was investigated experimentally. The ultimate strength increased by 87.5 %, and the dissipated energy increased by 89% when using staggered spiral stirrups and stirrups spacing was 20 mm. The results found that applying staggered spiral stirrups increased the cracking strength increased by 50%. However, there was a slight effect on the torsional stiffness of the beam. Also, the ultimate torque was affected by the amount of the transverse reinforcement. It was found that decreasing the stirrup spacing increased the ultimate torque. In addition, the torsional stresses and deformations of the reinforced concrete beams were enhanced by increasing the shear reinforcement. Applying the spiral stirrup confinement to the section decreases the twist angle. The present research design recommendation for RC-Beam could be summarized and illustrated in the next flow chart (Figure 38).

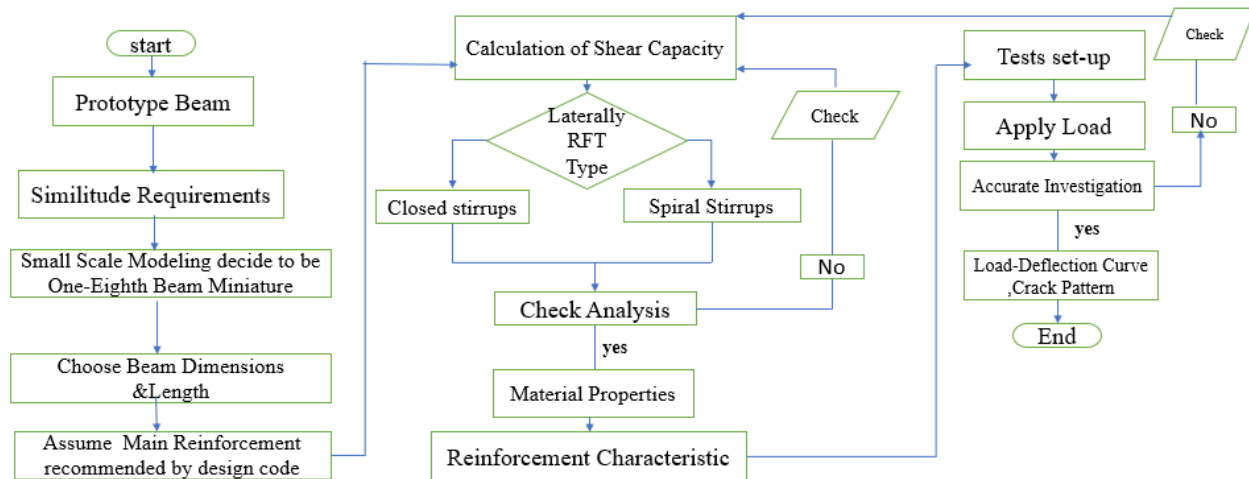


Figure 38. Flowchart of the stirrups methodology

8. Declarations

8.1. Author Contributions

Conceptualization, SH.M. and A.Y.; methodology, SH.M. and A.Y.; validation, SH.M., A.Y., and H.S.; formal analysis, SH.M.; investigation, H.S.; resources, SH.M. and H.S.; data curation, A.Y. and H.S.; writing—original draft preparation, SH.M.; writing—review and editing, SH.M.; visualization, A.Y. and H.S.; supervision, A.Y. and H.S.; project administration, SH.M.; funding acquisition, SH.M., A.Y. and H.S. All authors have read and agreed to the published version of the manuscript.

8.2. Data Availability Statement

The data presented in this study are available in the article.

8.3. Funding and Acknowledgements

The authors are grateful to the Civil Engineering Department of the Institute of Aviation of Engineering and Technology for financial support.

8.4. Conflicts of Interest

The authors declare no conflict of interest.

9. References

- [1] Sheikh, S. A., & Toklucu, M. T. (1993). Reinforced concrete columns confined by circular spirals and hoops. *ACI Structural Journal*, 90(5), 542–553. doi:10.14359/3949.
- [2] Park, R., & Paulay, T. (1975). *Reinforced Concrete Structures*, John Wiley & Sons, Hoboken, United States. doi:10.1002/9780470172834.
- [3] Kani, G. N. J. (1966). Basic Facts Concerning Shear Failure. *ACI Journal Proceedings*, 63(6), 675–692. doi:10.14359/7644.
- [4] Carpinteri, A., & Corrado, M. (2010). Dimensional analysis approach to the plastic rotation capacity of over-reinforced concrete beams. *Engineering Fracture Mechanics*, 77(7), 1091–1100. doi:10.1016/j.engfracmech.2010.02.021.
- [5] Christianto, D., Makarim, C. A., Tavio, & Liucius, Y. U. (2020). Size effect on shear stress of concrete beam without coarse aggregate. *Journal of Physics: Conference Series*, 1477(5), 52043. doi:10.1088/1742-6596/1477/5/052043.
- [6] Al-Zaidaneen, H., Murad, Y., Jaber, M. A., & Shatarat, N. (2022). Shear Strength of Light-Weight Reinforced Concrete Beams with Continuous Rectangular Spiral Reinforcement. *International Journal of Civil Engineering*, 20(3), 291–303. doi:10.1007/s40999-021-00667-z.
- [7] MohamedSalih, M. M., & Yousif, A. R. (2022). Effect of type, amount and configuration of reinforcement in HSC box-girders reinforced with BFRP bars and steel stirrups under torsion-shear-bending. *Ain Shams Engineering Journal*, 13(6), 101787. doi:10.1016/j.asej.2022.101787.
- [8] Ibrahim, A., Askar, H. S., & El-Zoughiby, M. E. (2022). Experimental and Numerical Nonlinear Analysis of Hollow RC Beams Reinforced with Rectangular Spiral Stirrups under Torsion. *Iranian Journal of Science and Technology - Transactions of Civil Engineering*, 46(6), 4019–4029. doi:10.1007/s40996-022-00852-7.

- [9] Hussain, H. K., Zewair, M. S., & Ahmed, M. A. (2022). High Strength Concrete Beams Reinforced with Hooked Steel Fibers under Pure Torsion. *Civil Engineering Journal (Iran)*, 8(1), 92–104. doi:10.28991/CEJ-2022-08-01-07.
- [10] Haroon, M., Koo, S., Shin, D., & Kim, C. (2021). Torsional behavior evaluation of reinforced concrete beams using artificial neural network. *Applied Sciences (Switzerland)*, 11(10), 4465. doi:10.3390/app11104465.
- [11] Fawzy, K., & Farouk, M. A. (2021). Torsion Strengthening of RC Beams with External Lateral Pressure Using Steel Plates. *Iranian Journal of Science and Technology - Transactions of Civil Engineering*, 45(3), 1413–1425. doi:10.1007/s40996-020-00536-0.
- [12] Shatarat, N., Hunifat, R., Murad, Y., Katkhuda, H., & Abdel Jaber, M. (2020). Torsional capacity investigation of reinforced concrete beams with different configurations of welded and unwelded transverse reinforcement. *Structural Concrete*, 21(2), 484–500. doi:10.1002/suco.201900054.
- [13] Katkhuda, H. N., Shatarat, N. K., & AL-Rakhameen, A. A. (2019). Improving the Torsional Capacity of Reinforced Concrete Beams with Spiral Reinforcement. *International Journal of Structural and Civil Engineering Research*, 8(2), 113–118. doi:10.18178/ijscer.8.2.113-118.
- [14] Ibrahim, A., Askar, H. S., & El-Zoughiby, M. E. (2022). Torsional behavior of solid and hollow concrete beams reinforced with inclined spirals. *Journal of King Saud University - Engineering Sciences*, 34(5), 309–321. doi:10.1016/j.jksues.2020.10.008.
- [15] Joh, C., Kwahk, I., Lee, J., Yang, I. H., & Kim, B. S. (2019). Torsional behavior of high-strength concrete beams with minimum reinforcement ratio. *Advances in Civil Engineering*, 2019. doi:10.1155/2019/1432697.
- [16] Rashidi, M., & Takhtfiroozeh, H. (2017). The Evaluation of Torsional Strength in Reinforced Concrete Beam. *Mechanics, Materials Science & Engineering Journal*, 7. doi:10.13140/RG.2.2.16568.75521.
- [17] Abdel-kareem, A. H., & Salam, A. M. A. El. (2020). Experimental and Analytical Investigation of Reinforced Concrete Beams with Large Web Opening under Pure Torsion. *International Journal of Advanced Engineering, Management and Science*, 6(1), 18–33. doi:10.22161/ijaems.61.4.
- [18] Tudu, C. (2012). Study of torsional behaviour of rectangular reinforced concrete beams wrapped with GFRP. National Institute of technology, Rourkela, India.
- [19] Othman, I., Meleka, N., Heiza, khaled, & Nabil, A. (2021). Behavior of Reinforced Concrete Beams Strengthened By GFRP Composites Subjected to Combined Bending and Torsion – Experimental Study. *ERJ. Engineering Research Journal*, 44(3), 295–302. doi:10.21608/erjm.2021.78234.1098.
- [20] Jariwala, V. H., Patel, P. V., & Purohit, S. P. (2013). Strengthening of RC beams subjected to combined torsion and bending with GFRP composites. *Procedia Engineering*, 51, 282–289. doi:10.1016/j.proeng.2013.01.038.
- [21] Khalil, G. I., Debaiky, A. S., Makhlof, M. H., & Ewis, E. A. E. S. (2017). Torsional behavior of reinforced concrete beams repaired or strengthened with transversal external post-tension elements. *International Journal of Science Technology & Engineering*, 4(4), 54-73.
- [22] Kandekar, S. B., & Talikoti, R. S. (2018). Study of torsional behavior of reinforced concrete beams strengthened with aramid fiber strips. *International Journal of Advanced Structural Engineering*, 10(4), 465–474. doi:10.1007/s40091-018-0208-y.
- [23] Habeeb Askandar, N., & Darweesh Mahmood, A. (2020). Torsional Strengthening of RC Beams with Near-Surface Mounted Steel Bars. *Advances in Materials Science and Engineering*, 2020, 1–11. doi:10.1155/2020/1492980.
- [24] Ghobarah, A., Ghorbel, M. N., & Chidiac, S. E. (2002). Upgrading Torsional Resistance of Reinforced Concrete Beams Using Fiber-Reinforced Polymer. *Journal of Composites for Construction*, 6(4), 257–263. doi:10.1061/(asce)1090-0268(2002)6:4(257).
- [25] ECP-203. (2020). Egyptian code for design and construction of reinforced concrete structures. National Housing and Building Research Center, Giza, Egypt.
- [26] ACI 318-08. (2008). Building Code Requirements for Structural Concrete and Commentary. American Concrete Institute, Farmington Hills. United States.
- [27] EN 1992-1-1. (2005). Eurocode 2: Design of Concrete Structures: General Rules and Rules for Buildings. In British Standard Institution. British Standard Institution, London, United Kingdom.
- [28] Noor, F. A., & Boswell, L. F. (1992). Small scale modelling of concrete structures. CRC Press, Boca Raton, United States. doi:10.1201/9781482286700.
- [29] JSCE No-15. (2007). Standard specifications for concrete structures-2007. Design. Japan Society of Civil Engineers, Tokyo, Japan.